Response of an oscillator with a Duffing parameter of the fifth power

K. Al-Zubi

Technische Universiteit Delft

TU Delft Delft University of Technology

Response of an oscillator with a Duffing parameter of the fifth power

by

K. Al-Zubi

in partial fulfillment of the requirements for the degree of

Bachelor of Science
in Applied Physics

at the Delft University of Technology,
to be defended publicly on 19-03-2019.

Supervisor:	Prof. Ya. M. Blanter	
Thesis committee:	Dr. M. Blaauboer,	TU Delft

Delft University of Technology

Abstract

Quintic Duffing oscillator is considered. Amplitude-phase relations are derived using averaging theorem and perturbation methods. First The forced quintic system is studied. Stability regions are compared to the general case with quintic-qubic non-linearity. Numerical results show that Perturbation method and averaging are in agreement with each other for a range of frequency values. For first order perturbation the Lindstedt-Poincaré technique is reduced to the multiple scales method. Only when both linearities are taken into account, five solutions are present. Magnitudes of non-linearity input plays a role in observing region of unstable solutions.

Contents

1

Introduction

Non-linear dynamical systems are intensely studied to describe many physical phenomena. One of these physical applications where non-linearity shows up are the nano-mechanical systems such as Carbon nano tube (CNT) experiments. A carbon nano tube (CNT) is a stiff, bottom-up nano mechanical resonator with a large aspect ratio [1]. A quantum dot experiences a restoring force with single non-linearity term known as the 'Duffing parameter' [2] due to single-electron tunnelling. In order to understand the physical behaviour of such systems, the Duffing equation must be studied and the amplitude-phase relation (frequency response) must be obtained. For more details about different topics such as bifurcations, stable regions, numerical calculations and chaos of cubic Duffing oscillator, the reader is advised to [3-6].

We start this thesis by reviewing the concept of linear equations and compare it to non-linear systems. Once a short review is given, the quintic Duffing equation with fifth power non-linearity is reviewed. First the unforced equation is investigated by defining the force and its potential. Once the expression of the total energy is given, the Hamilton equations are formulated. Studying the potential curves shows that for some input parameters, unbounded solutions can occur. The concept local stability is studied and stable regions are proved using Jacobi stability analyses for a given damping magnitude. After a general investigation of the unforced system, we arrive at the core of this thesis. The forced Duffing equation with fifth power non-linearity is studied. Several methods are used in order to obtain the amplitude-phase relation at which useful conclusions can be drawn. the research question is: how many solutions does a quintic non-linearity provide for a given frequency value? And how do such solutions behave under varying input parameters.

The first method applied for the frequency response is the averaging theorem. This is done by using the Van der Pol transformation. To eliminate trigonometric secularities, The definition of averaging applied. After the system is reduced to a simpler form, the transformation to polar coordinate is made to finally obtain expressions for the amplitude and phase equation.

To compare the results obtained by averaging theorem, the Perturbation method is introduced. Perturbation methods are widely used in solving countless dynamical systems [7,8]. First the multiple scales technique will be outlined and the introduced fast and low scales will be explained. an improved version of the classical multiple scales method is the Lindstedt-Poincaré. Frequency response is calculated by both techniques and is compared to the result obtained averaging. Before numerical calculation are presented, the general case of the cubic-quintic Duffing equation is investigated. The Hamiltonian is formulated for the system containing both linearities and the frequency response is calculated. At the end numerical calculations are presented for all cases and methods. The input parameters are varied and useful conclusions about stability regions are made.

In the course of writing this these, I received frequent and close supervision from Prof. Ya. M. Blanter and would like to thank him sincerely for guiding me through the process and giving comments on my progress.

The numerical solutions and the corresponding graphs are obtained by the program Matlab 2018©. The written text, formulas and figures in this paper are generated using the TEX engine typesetting XƎLATEX.

K. Al-Zubi
Delft, March 2019

2

Theory

2.1. Linear and non-linear equations

The focus in this report will be on second order differential equations since the main function to solve is the Duffing equation.

A second order differential equation has the following form:

$$\frac{d^2x}{dt^2} = f\left(t, x, \frac{dx}{dt}\right). \tag{2.1}$$

Eq. (2.1) is said to be linear if it has the form

$$f\left(t, x, \frac{dx}{dt}\right) = g(t) - p(t)\frac{dx}{dt} - q(t)x, \tag{2.2}$$

that is, if f is linear in x and $\frac{dx}{dt}$. A physical example of a linear differential equation is the Simple harmonic oscillator. Such equations have analytical solutions which can be found by several common ways.

Recall that a system of coupled linear equations has the form:

$$\dot{x} = Ax \qquad x \in \mathbb{R}^n \tag{2.3}$$

A is a $n \times n$ matrix with constant coefficients. The solution of such systems can be found by finding the eigenvalues and the generalized eigenvectors.

A second order differential equation is in general non-linear. Linearity is property of which well-defined solutions are known. For most non-linear equations no exact solution is known. It is the task to find approximate methods to determine the solution.

2.2. Duffing oscillator

The most simplified form of the Duffing's equation is the following:

$$\ddot{x} + \delta\dot{x} + \beta x + \alpha x^3 = \gamma \cos \omega t. \tag{2.4}$$

Eq. (2.4) is often used to describe driven and damped oscillators such as a beam moving under forced vibrations. The Duffing's equation does not guarantee a solution of the physical problem, it is rather an approximate model.

The given numbers are the relevant parameters and each one has a physical meaning. δ controls the amount of damping, β measures the stiffness of the linear force, α is the amount of non-linearity of the restoring force (also known as the Duffing parameter), γ is the amplitude of the periodic driven force and ω is the driven frequency.

The aim in this thesis is to solve the quintic Duffing equation. The term "quintic" stands for fifth power x^5. There have been a lot of papers dealing with cubic non-linearity x^3, therefore the amplitude-phase relation for this system are known already. Another reason is to check whether the outcomes of such parameter are relevant for the results in the experimental model. At some point in the experiment the Duffing parameter x^3 vanishes as the gate voltage drops down. The voltage function does explicitly depend on the the non-linear parameter and therefore it is affected by such drop. It is now the task to see whether changing the non-linear parameter would give a total different outcome.

The quintic Duffing equation has the following form:

$$\ddot{x} + \delta\dot{x} + \beta x + \alpha x^5 = \gamma \cos \omega t \tag{2.5}$$

Before Eq. (2.5) is investigated, the case where α and β are real numbers is studied.

3

The unforced system

In the case where damping and external force are absent ($\delta = \gamma = 0$) the system is reduced to:

$$\ddot{x} + \beta x + \alpha x^5 = 0. \tag{3.1}$$

Eq. (3.1) represents an equation of motion. Since the dimensions are expressed in length-units ,α should have units $[\sim \frac{1}{m^4}]$ to compensate for the x^5 term.

The force as a function of displacement from equilibrium is

$$F(x) = -\beta x - \alpha x^5. \tag{3.2}$$

The parameter x is considered to be a one dimensional model for simplicity. One can think of the problem being three-dimensional and replace x by the vector $\mathbf{r} = (\mathbf{x}, \mathbf{y}, \mathbf{z})$ and there will be no major differences. Note that if the Duffing parameter would vanish, the force will become linear and the system is reduced to a simple harmonic motion.

It is known from classical mechanics that the force is defined as the gradient of the potential energy

$$F(\mathbf{r}) = -\nabla V(\mathbf{r}) \tag{3.3}$$

and from Eq. (3.2) Follows that the potential energy is given by the following expression:

$$V(x) = \frac{\beta}{2}x^2 + \frac{\alpha}{6}x^6 \tag{3.4}$$

Rewriting Eq. (3.1) in terms of generalised coordinates to form the Hamiltonian

$$\dot{u} = v = \frac{\partial H}{\partial v} \tag{3.5}$$

$$\dot{v} = -\beta u - \alpha u^5 = -\frac{\partial H}{\partial u} \tag{3.6}$$

Eq. (3.5) and Eq. (3.6) are known as the Hamilton's equations, where

$$H = \frac{1}{2}v^2 + \frac{\beta}{2}u^2 + \frac{\alpha}{6}u^6. \tag{3.7}$$

Note that ($H = T + V = \text{Energy}$) and since it does not depend explicitly on time the energy is a conserved quantity.

For a better understanding of the physical quantities, the potential function and the associated force are analysed. For different values of α and β, several plots are shown in figure 1.

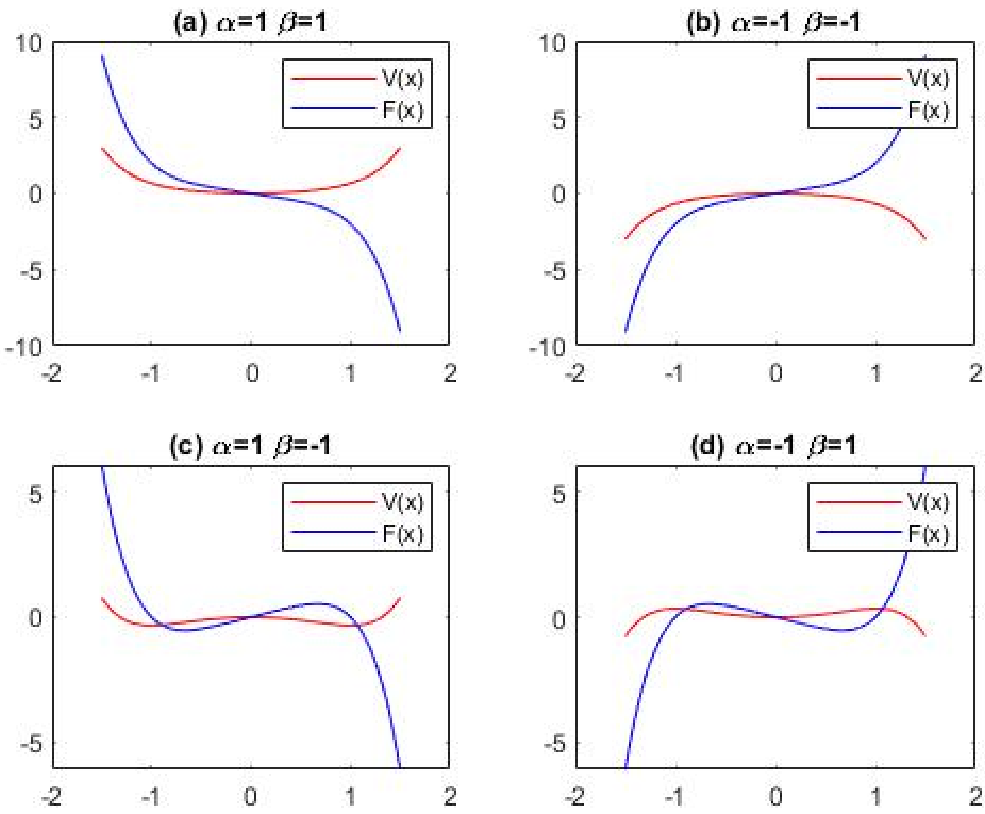

Figure 3.1: Potential and force of the undamped system for different values of α and β

In the first case $\alpha, \beta = 0$ we can see the potential function is similar to that of the harmonic oscillator, except that for large values of x the x^6 term will dominate. For the second case we expect same behaviour as when $\alpha = 0, \beta < 0$ which does not seem interesting. The cases (c) and (d) are more interesting, we see two additional points when $F = 0$ which are different from when $x = 0$. Again, for large values of x the potential will be dominated by the x^6 term. The situation sketched in (c) shows that the system is bounded while in (d) it is unbounded as solutions will diverge into $\pm\infty$. In the next section stability will be studied in more depth.

3.1. Local stability

If a small amount of damping is present, the Hamiltonian equations becomes:

$$\dot{u} = v \tag{3.8}$$

$$\dot{v} = +\beta u - \alpha u^5 - \delta v \qquad \alpha, \beta, \delta > 0 \tag{3.9}$$

The considered case is $(\alpha = 1, \beta = -1)$, for which the sign of β became positive in Eq. (3.9). For this two-dimensional system the equilibria must satisfy $\dot{u} = \dot{v} = 0$. A little calculations shows that there are three equilibria points, one at the origin $(u, v) = (0, 0)$ and two other points at $(u, v) = (\pm(\frac{\beta}{\alpha})^{\frac{1}{4}}, 0)$. For a system with coupled differential equations one can find the critical points by finding the eigenvalues. The Jacobian matrix is defined as follows

$$\begin{bmatrix} \frac{\partial \dot{u}}{\partial u} & \frac{\partial \dot{u}}{\partial v} \\ \frac{\partial \dot{v}}{\partial u} & \frac{\partial \dot{v}}{\partial v} \end{bmatrix} \tag{3.10}$$

$$\begin{bmatrix} 0 & 1 \\ -\beta & -\delta \end{bmatrix} \quad (0,0) \qquad \begin{bmatrix} 0 & 1 \\ -4\beta & -\delta \end{bmatrix} \quad (\pm\sqrt[4]{\frac{\beta}{\alpha}}, 0).$$

The first case at the origin, the eigenvalue equation reads:

$$\lambda^2 + \delta\lambda - \beta = 0 \tag{3.11}$$

The eigenvalue can be solved by the method of 'completing the square' and its value is:

$$\lambda = -\frac{\delta}{2} \pm \frac{\sqrt{\delta^2 + 4\beta}}{2} \tag{3.12}$$

When there is no damping λ is simply $\pm\sqrt{\beta}$. Two real eigenvalues with different signs, which indicates that (0,0) is a saddle point. This is an additional case when $\delta \neq 0$. It is easy to see that $\sqrt{\delta^2 + 4\beta} > \delta$ which means a saddle. The second eigenvalue equation reads

$$\lambda^2 + \delta\lambda + 4\beta = 0, \tag{3.13}$$

for the eigenvalues, the expression

$$\lambda = -\frac{\delta}{2} \pm \frac{\sqrt{\delta^2 - 16\beta}}{2} \tag{3.14}$$

λ is now $\pm 2\sqrt{-\beta}$ when $\delta = 0$. The nature of the critical points is a centre point since the two values are imaginary with zero real part. If friction is present, either two real negative eigenvalues or two imaginary with negative real part are obtained, which in both cases is asymptotically stable. Thus, for all eigenvalues it is proven that the system ($\alpha = 1, \beta < 0$) is stable.

4

The forced system

There are several ways one can use to determine the frequency response of a time dependent forced system. The technique that will be used in this thesis is called Averaging.

4.1. Averaging method

Averaging is a technique of replacing a vector field by its average to obtain periodic solutions. Given a function $f(t)$, one can find its average using the following definition

$$\langle f \rangle = \frac{1}{T}\int_0^T f(t)\mathrm{d}t \tag{4.1}$$

in our case averaging is useful and reduces the number of calculation steps. By averaging over a period of $\frac{2\pi}{\omega}$ the system becomes time-invariant and is easier to work with compared to the original system.

It is sometimes useful to do transformations in order to simplify problem. Van der Pol transformation is used to transform from one basis to another. One can think of The Duffing equation being spanned by the basis(vectors) x and $\dot{x}$. This idea will be more intuitive if we plot the velocity as a function of displacement.

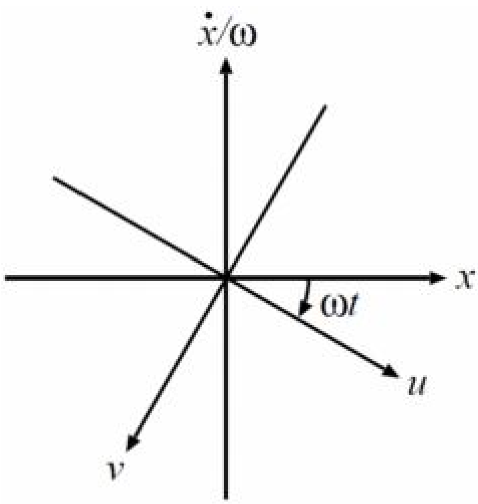

Figure 4.1: Van der Pol transformation in a 2-D plane[2].

Fig. 4.1 shows the u axis being rotated clockwise with angle frequency ω to obtain new basis vectors. The new basis vectors (u, v) can be written in terms of $(x, \dot{x})$ and vice versa (inverse transformation).

From a geometrical point of view, it should be trivial to write down both components of (u, v) just by looking at Fig. 4.1. An alternative way is to use Rotational matrix.

$$\mathrm{R}\mathbf{x} = \mathbf{u} = \begin{bmatrix} \cos\omega t & -\sin\omega t \\ -\sin\omega t & -\cos\omega t \end{bmatrix} \begin{bmatrix} x \\ \dot{x} \end{bmatrix} = \begin{bmatrix} u \\ v \end{bmatrix} \tag{4.2}$$

To calculate the inverse transformation one should find the inverse matrix R^{-1}. Note that the matrix R itself is orthogonal i.e. spanned by orthonormal basis vectors. From matrix Algebra we know that for an orthogonal matrix the inverse is equal to its hermitian transpose $\mathrm{R}^{-1} = \mathrm{R}^{\dagger}$.

$$\mathrm{R}^{\dagger}\mathbf{u} = \mathbf{x} = \begin{bmatrix} \cos\omega t & -\sin\omega t \\ -\sin\omega t & -\cos\omega t \end{bmatrix} \begin{bmatrix} u \\ v \end{bmatrix} = \begin{bmatrix} x \\ \dot{x} \end{bmatrix} \tag{4.3}$$

The four equations become:

$$u = (x)\cos\omega t - \left(\frac{\dot{x}}{\omega}\right)\sin\omega t \tag{4.4}$$

$$v = -(x)\sin\omega t - \left(\frac{\dot{x}}{\omega}\right)\cos\omega t \tag{4.5}$$

$$x = (u)\cos\omega t - (v)\sin\omega t \tag{4.6}$$

$$\frac{\dot{x}}{\omega} = -(u)\sin\omega t - (v)\cos\omega t \tag{4.7}$$

Eq. (4.4) and Eq. (4.5) are spanned by the basis vectors $x, \frac{\dot{x}}{\omega}$. Once expressions for $x, \frac{\dot{x}}{\omega}$ are calculated using Eq. (4.6) and Eq. (4.7), the acceleration $\ddot{x}$ can be evaluated:

$$\begin{aligned} \dot{x} = (\dot{u})\cos\omega t - (u)\omega sin\omega t - (\dot{v})\sin\omega t - (v)\omega\cos\omega = \omega\big(-(u)\sin\omega t - (v)\cos\omega t\big) \\ \dot{x} = -(u)\omega\sin\omega t - (v)\omega\cos\omega t \end{aligned} \tag{4.8}$$

$$\ddot{x} = -(\dot{u})\omega\sin\omega t - (u)\omega^2\cos\omega t - (\dot{v})\omega\cos\omega t + (v)\omega^2\sin\omega t \tag{4.9}$$

Note that x,$\dot{x}$ and $\ddot{x}$ are now written as a linear combination of (u, v). The aim is to find a final expression with only these parameters. Filling Eq. (4.8) and Eq. (4.9) in Eq. (2.5) results in:

$$\begin{aligned} -(\dot{u})\omega\sin\omega t - (u)\omega^2\cos\omega t - (\dot{v})\omega\cos\omega t + (v)\omega^2\sin\omega t \\ + \delta(-(u)\omega\sin\omega t - (v)\omega\cos\omega t) \\ + \beta((u)\cos\omega t - (v)\sin\omega t) \\ + \alpha((u\cos\omega t)^5 - 5(u\cos\omega t)^4(v\sin\omega t) + 10(u\cos\omega t)^3(v\sin\omega t)^2 \\ - 10(u\cos\omega t)^2(v\sin\omega t)^3 + 5(u\cos\omega t)(v\sin\omega t)^4 - (v\sin\omega t)^5) - \gamma\cos\omega t = 0 \end{aligned} \tag{4.10}$$

At the current stage Eq. (4.10) seems to be too complicated to rewrite in other form due to multiplication of higher order trigonometric functions. In order to reduce Eq. (4.10) to simpler expression without loosing any necessary information, averaging will be applied. This is done in two steps. First Eq. (4.10) is multiplied with $\sin\omega t$:

$$\begin{aligned} \dot{u}\omega\sin^2\omega t = \sin\omega t\big\{ - (\dot{v})\omega\cos\omega t - (u)\omega^2\cos\omega t + (v)\omega^2\sin\omega t \\ + \delta(-(u)\omega\sin\omega t - (v)\omega\cos\omega t) + \beta((u)\cos\omega t - (v)\sin\omega t) \\ + \alpha((u\cos\omega t)^5 - 5(u\cos\omega t)^4(v\sin\omega t) + 10(u\cos\omega t)^3(v\sin\omega t)^2 \\ - 10(u\cos\omega t)^2(v\sin\omega t)^3 + 5(u\cos\omega t)(v\sin\omega t)^4 - (v\sin\omega t)^5) - \gamma\cos\omega t\big\} \end{aligned} \tag{4.11}$$

The second step is to multiply Eq. (4.10) with $\cos \omega t$:

$$\begin{aligned}\dot{u}\omega\cos^2 \omega t = \cos \omega t\{&-(\dot{v})\omega \cos \omega t - (u)\omega^2 \cos \omega t + (v)\omega^2 \sin \omega t \\ &+ \delta(-(u)\omega\sin \omega t - (v)\omega\cos \omega t) + \beta((u) \cos \omega t - (v) \sin \omega t) \\ &+ \alpha((u \cos \omega t)^5 - 5(u \cos \omega t)^4 (v \sin \omega t) + 10(u \cos \omega t)^3 (v \sin \omega t)^2 \\ &- 10(u \cos \omega t)^2 (v \sin \omega t)^3 + 5(u \cos \omega t)(v \sin \omega t)^4 - (v \sin \omega t)^5) - \gamma \cos \omega t\}.\end{aligned} \tag{4.12}$$

Now the definition(Eq. (4.1)) of averaging can be applied to Eq. (4.11) and Eq. (4.12).

$$\langle \sin^2 \omega t\rangle = \frac{1}{T}\int_0^T \sin^2 \omega t \mathrm{d}t = \frac{1}{T}\int_0^T \frac{1}{2}\mathrm{d}t - \frac{1}{T}\int_0^T \frac{\cos 2\omega t}{2}\mathrm{d}t. \tag{4.13}$$

Using integration by substitution, the outcome $\langle \sin^2 \omega t\rangle = \frac{1}{2}$ is found. For the other terms the same integral method is used and the outcomes are the following expressions:

$$\langle \sin^2 \omega t\rangle = \langle \cos^2 \omega t\rangle = \frac{1}{2} \tag{4.14}$$

$$\langle \sin \omega t \cos \omega t\rangle = \langle \sin \omega t \cos^5 \omega t\rangle = \langle \sin^3 \omega t \cos^3 \omega t\rangle = \langle \sin^5 \omega t \cos \omega t\rangle = 0 \tag{4.15}$$

$$\langle \cos^4 \omega t \sin^2 \omega t\rangle = \langle \sin^4 \cos^2 \omega t\rangle = \frac{1}{16} \tag{4.16}$$

$$\langle \sin^6 \omega t\rangle = \langle \cos^6 \omega t\rangle = \frac{5}{16} \tag{4.17}$$

The system is now reduced to the following expressions:

$$\dot{u}\omega = v\omega^2 - \delta(u)\omega - \beta v - \frac{5\alpha}{8}(u^2 + v^2)^2 v \tag{4.18}$$

$$\dot{v}\omega = -u\omega^2 - \delta(v)\omega + \beta u + \frac{5\alpha}{8}(u^2 + v^2)^2 u - \gamma. \tag{4.19}$$

The next task is to plot the amplitude-phase diagram. We introduce the polar coordinates:

$$u(t) = r(t) \cos \phi(t) \qquad v(t) = r(t) \sin \phi(t). \tag{4.20}$$

To rewrite the solutions in terms of polar coordinates $r = \sqrt{u^2 + v^2}$ and $\phi = \arctan\left(\frac{v}{u}\right)$, differentiation with respect to t is applied using the chain rule:

$$\dot{r} = \frac{1}{r}[u\dot{u} + v\dot{v}] \tag{4.21}$$

$$\dot{\phi} = \frac{1}{1 + \frac{v^2}{u^2}}\left(-\frac{v\dot{u}}{u^2} + \frac{\dot{v}}{v}\right). \tag{4.22}$$

Evaluating Eq. (4.21) and Eq. (4.22)

$$\dot{r} = \frac{1}{r}\left[-\delta\omega u^2 + \Omega v u - \frac{5\alpha}{8}(u^2 + v^2)^2 v u - \Omega u v - \delta\omega v^2 - \frac{5\alpha}{8}(u^2 + v^2)^2 v u - \delta v\right] \tag{4.23}$$

$$\dot{\phi} = \frac{1}{\omega r^2}\left[-\Omega u^2 - \delta\omega v u + \frac{5\alpha}{8}(u^2 + v^2)u^2 - \delta u - \Omega v^2 + \delta\omega v u + \frac{5\alpha}{8}(u^2 + v^2)v^2\right] \tag{4.24}$$

gives the amplitude-phase relation:

$$\dot{r} = \frac{-1}{\omega}(\delta\omega r + \gamma \sin \phi) \tag{4.25}$$

$$\dot{\phi} = \frac{1}{\omega}\left(-\Omega + \frac{5\alpha}{8}r^4 - \frac{\gamma \cos \phi}{r}\right) \tag{4.26}$$

where $\Omega = \omega^2 - \beta$.

Recall that $x(t) = r(t)\cos(\omega t + \phi)$, this means that the solutions $r(t)$ and $\phi(t)$ are respectively the amplitude and phase of the real solution. Both $r(t), \phi(t)$ are time depended, which implies that small changes will occur over time to both quantities. For steady-state solution, time derivatives will set equal to zero ($\dot{r}(t) = \dot{\phi}(t) = 0$). An easy trick to combine Eq. (4.25) and Eq. (4.26) is to use the Pythagorean identity $\cos^2\phi + \sin^2\phi = 1$. This results in the following expression:

$$-\gamma^2 + \frac{25\alpha^2}{64}(r^2)^5 + \frac{5}{4}\alpha\beta(r^2)^3 - \frac{5}{4}\alpha\omega^2(r^2)^3 + \left(\omega^4 - 2\omega^2\beta + \beta^2 + \delta^2\omega^2\right)(r^2) = 0 \tag{4.27}$$

Eq. (4.27) can be rearranged as

$$(r^2)\omega^4 + \left(\delta^2 - \frac{5}{4}\alpha(r^2)^2 - 2\beta\right)(r^2)\omega^2 + \left[-\gamma^2 + \frac{25\alpha^2}{64}(r^2)^5 + \frac{5}{4}\alpha\beta(r^2)^3 + \beta^2 r^2\right] = 0 \tag{4.28}$$

Note that Eq. (4.28) is a polynomial of fourth power:

$$A\omega^4 + B\omega^2 + C = 0 \tag{4.29}$$

where

$$A = r^2 \tag{4.30}$$

$$B = \left(\delta^2 - \frac{5}{4}\alpha(r^2)^2 - 2\beta\right)(r^2) \tag{4.31}$$

$$C = -\gamma^2 + \frac{25\alpha^2}{64}(r^2)^5 + \frac{5}{4}\alpha\beta(r^2)^3 + \beta^2 r^2. \tag{4.32}$$

ω values can be solved by completing the square, and we 4 solutions are expected:

$$\omega^2 = \frac{-B \pm \sqrt{B^2 - 4AC}}{2A} \tag{4.33}$$

alternatively as

$$\omega = \pm\sqrt{\frac{-B \pm \sqrt{B^2 - 4AC}}{2A}} \tag{4.34}$$

Eq. (4.28) will guarantee 4 solutions as expected. These solutions yield real values provided

$$B^2 - 4AC \geqslant 0 \tag{4.35}$$

and also

$$-B \pm \sqrt{B^2 - 4AC} \geqslant 0 \tag{4.36}$$

Since an expression for the frequency is obtained, it is now possible to present an amplitude-phase diagram to analyse the region of stability and jump-ups phenomena.

4.2. Perturbation Theorem

Perturbation methods proved to be useful in finding approximate analytical solutions for many physical applications. The general idea of such method is to write a solution which is expanded in power series. By doing so, problems which are impossible to solve analytically become solvable. In the case of the duffing non-linearity, this method works well and guarantees acceptable solutions compared to the numerical solutions. the final solution has the following form:

$$X = X_0 + \epsilon X_1 + \epsilon^2 X_2 + ... = \sum_{n=0}^{\infty} \epsilon^n X_n \tag{4.37}$$

where X_0 is the leading term and is often an exact solution of another simpler system. For example, a solution of the simple harmonic motion (as we'll see), which is the simplest case when $\alpha = 0$. The $X_1, X_2, ..$ are higher order terms and describe the deviation in the solution. ϵ is the perturbation parameter and has a value between 0 and 1.

There are many perturbation methods one can think of when dealing with non-linear dynamics. However, in this research only two techniques will be studied. The classical multiple scales method, the starting point of this topic. The amplitude-phase relations for the quintic Duffing oscillator will be calculated. The same will be done using the Lindstedt-Poincaré method and both results will be compared. Both methods are used for the forced system and are based on eliminating secularities which will become more clear.

4.2.1. Multiple scales

Consider the follwing Duffing equation with first order perturbation correction:

$$\ddot{x} + x + \epsilon\delta\dot{x} + \epsilon\alpha x^5 = \epsilon f \cos \Omega t \tag{4.38}$$

where f is the external applied force and ϵ is the small perturbation parameter. For the angular frequency the notation Ω is used instead of ω. Eq. (4.38) is known as "first order perturbation" equation. The nth perturbation correction stands for the power of ϵ.

We start the multiple scale analysis by introducing the slow and the fast scales:

$$T_0 = t, \quad T_1 = \epsilon t \tag{4.39}$$

where T_0, T_1 are the slow and fast scales respectively. By introducing such transformation, we switch from the time independence parameter t to a new independent parameters T_0, T_1. Since the displacement depends implicitly on time, $\{\dot{x}, \ddot{x}\}$ should be recalculated using the chain rule. Calculating the time derivatives with respect to these variables using the chain rule:

$$\frac{\mathrm{d}}{\mathrm{d}t} = D_0 + \epsilon D_1 + ... \tag{4.40}$$

$$\frac{\mathrm{d}^2}{\mathrm{d}t^2} = D_0^2 + 2\epsilon D_0 D_1 + ... \tag{4.41}$$

where $D_n^j = \frac{\partial^j}{\partial T_n^j}$. Once the transformation is performed, the approximate solution

$$x = x_0(T_0, T_1) + \epsilon x_1(T_0, T_1) + ... \tag{4.42}$$

is inserted in Eq. (4.38). Equal powers of ϵ are collected and ϵ is chosen to be 1:

$$O(\epsilon^0): \qquad D_0^2 x_0 + x_0 = 0 \tag{4.43}$$

$$O(\epsilon^1): \qquad D_0^2 x_1 + x_1 = -2D_0 D_1 x_0 - \delta D_0 x_0 - \alpha {x_0}^5 + f \cos \Omega T_0 \tag{4.44}$$

From Eq. (4.43) we find the unperturbed solution:

$$x_0 = Ae^{iT_0} + c.c = a\cos(T_0 + \lambda) \tag{4.45}$$

where 'c.c' stands for the complex conjugate ($A^* e^{-iT_0}$). A is the complex amplitude:

$$A = \frac{a}{2}e^{i\lambda}. \tag{4.46}$$

Note that the first(unperturbed) solution is the exact solution for the harmonic oscillator. The non-linearity in the second solution will cause the amplitude and phase $a(t), \lambda(t)$ to change slowly over time. The unperturbed solution is inserted in the right-hand side of Eq. (4.44). For primary resonances we assume

$$\Omega = 1 + \epsilon\sigma \tag{4.47}$$

and eliminating secular terms yield

$$-2iD_1A - i\delta A - \alpha 10A^3A^{*2} + \frac{f}{2}e^{i\sigma T_1} = 0 \tag{4.48}$$

Secular terms are the terms which causes unphysical behaviour of the system. Such behaviour could be diverging and leads to unbounded growth in amplitude. By looking at Eq. (4.48), the complex conjugates parts are eliminated as well as the additional parts of x_0^5.

Evaluating the complex amplitude:

$$-2iD_1\left[\frac{a}{2}e^{i(\sigma T_1 - \gamma)}\right] - i\delta\frac{a}{2}e^{i\lambda} - \alpha\frac{10}{32}a^5e^{i\lambda} + \frac{f}{2}e^{i\lambda + i\gamma} = 0 \tag{4.49}$$

where the phase is defined to be

$$\gamma = \sigma T_1 - \lambda \tag{4.50}$$

note that $\lambda = \lambda(t)$, the differentiation operator D_1 acts on the exponential which results in the following expression:

$$(\sigma - \dot{\gamma})a - i\dot{a} - i\delta\frac{a}{2} - \alpha\frac{10}{32}a^5 + \frac{f}{2}\cos\gamma + i\frac{f}{2}\sin\gamma = 0 \tag{4.51}$$

seperation of the real and imaginary part gives the amplitude-phase relation:

$$\dot{a} = -\delta\frac{a}{2} + \frac{f}{2}\sin\gamma \tag{4.52}$$

$$\dot{\gamma} = \sigma - \alpha\frac{10}{32}a^4 + \frac{f}{2a}\cos\gamma \tag{4.53}$$

The amplitude-phase relation obtained by the multiple scales method is similar to the one obtained by the averaging theorem except for the multiplication factor $\frac{1}{2}$. This additional factor is due to the choice of the unperturbed solution. Instead of evaluating the real solution, the complex amplitude is used $A = \frac{a}{2}e^{i\lambda}$. As a result the amplitude will become $\frac{a}{2}$ instead of a, resulting in the $\frac{1}{2}$ difference factor.

4.2.2. Lindstedt-Poincaré

When the classical multiple scales analysis fails to produce valid physical solutions, several techniques can be used in order to avoid secularities (especially for strongly non-linear systems). One of the techniques that combines the multiple scale method and the Lindstedt-Poincaré techniques and will be outlined in the section. While the multiple scales method succeeded in producing amplitude-phase relation in the previous section, the Lindstedt-Poincaré method will be used to compare both methods and outcomes.

The main future of the Lindstedt-Poincaré method is to apply the time transformation

$$\tau = \omega t \tag{4.54}$$

and expanding the frequency in ϵ

$$\omega^2 = 1 + \epsilon\omega_1. \tag{4.55}$$

The leading frequency ω_0 is chosen to be one. The displacement x will depend on τ and the transformation

$$\frac{\partial x}{\partial t} = \frac{\partial x}{\partial \tau}\frac{\partial \tau}{\partial t}, \tag{4.56}$$

which will result in the following expressions:

$$\dot{x}(t) \longrightarrow \omega\dot{x}(\tau) \tag{4.57}$$

$$\ddot{x}(t) \longrightarrow \omega^2\ddot{x}(\tau) \tag{4.58}$$

The Duffing equation becomes

$$\omega^2\ddot{x} + x + \omega\epsilon\delta\dot{x} + \epsilon\alpha x^5 = \epsilon f \cos\frac{\Omega}{\omega}T_0, \tag{4.59}$$

where the slow and fast time scales are used

$$T_0 = \tau, \quad T_1 = \epsilon\tau. \tag{4.60}$$

The derivatives with respect to the new parameters are calculated

$$\frac{\mathrm{d}}{\mathrm{d}t} = D_0 + \epsilon D_1 + \dots \tag{4.61}$$

$$\frac{\mathrm{d}^2}{\mathrm{d}t^2} = D_0^2 + 2\epsilon D_0 D_1 + \dots \tag{4.62}$$

and the approximate solution

$$x = x_0(T_0, T_1) + \epsilon x_1(T_0, T_1) + \dots \tag{4.63}$$

are inserted in Eq. (4.59).

$$\omega^2\left(D_0^2 + 2\epsilon D_0 D_1\right)[x_0 + \epsilon x_1] + \left(\omega^2 - \epsilon\omega_1\right)[x_0 + \epsilon x_1] + \epsilon\delta\left(D_0 + \epsilon D_1\right)\omega[x_0 + \epsilon x_1] + \epsilon\alpha[x_0 + \epsilon x_1] = \epsilon f \cos\frac{\Omega}{\omega}T_0 \tag{4.64}$$

Collecting equal powers of ϵ gives the following expressions:

$$O(\epsilon^0): \quad \omega^2 D_0^2 x_0 + \omega^2 x_0 = 0 \tag{4.65}$$

$$O(\epsilon^1): \quad \omega^2 D_0^2 x_1 + \omega^2 x_1 = -2\omega^2 D_0 D_1 x_0 + \omega_1 x_0 - \delta\omega D_0 x_0 - \alpha {x_0}^5 + f\cos\frac{\Omega}{\omega}T_0 \tag{4.66}$$

Again, ϵ is chosen to be one since the expressions are obtained. The unperturbed equation (Eq. (4.65)) is a simple harmonic model which has the solution

$$x_0 = Ae^{iT_0} + c.c = a\cos(T_0 + \lambda) \tag{4.67}$$

$$A = \frac{a}{2}e^{i\lambda} \tag{4.68}$$

A is the complex amplitude. Filling the unperturbed solution in the right hand side Eq. (4.66) and eliminating secularities yield

$$-2i\omega^2 D_1 A + \omega_1 A - i\omega\delta A - \alpha 10 A^3 {A^*}^2 + \frac{f}{2}e^{i\sigma T_1} = 0. \tag{4.69}$$

By investigating Eq. (4.69), it is clear that ω_1 is a complexed valued parameter. This leads to unphysical behaviour and therefore the term $\omega_1 A$ should be eliminated as well. The next step is to evaluate the derivative operator $D_1 A$ and assuming

$$\gamma = \sigma T_1 - \lambda, \tag{4.70}$$

Eq. (4.69) becomes:

$$-2i\omega^2 D_1\left[\frac{a}{2}e^{i(\sigma T_1-\gamma)}\right] - i\delta\omega\frac{a}{2}e^{i\lambda} - \alpha\frac{10}{32}a^5 e^{i\lambda} + \frac{f}{2}e^{i\lambda+i\gamma} = 0. \tag{4.71}$$

The phase $\gamma = \gamma(t)$ depends implicitly on the parameter T_1. After multiplying all terms, this results in

$$(\sigma - \dot{\gamma})\omega^2 a - i\omega^2\dot{a} - i\delta\omega\frac{a}{2} - \alpha\frac{10}{32}a^5 + \frac{f}{2}\cos\gamma + i\frac{f}{2}\sin\gamma = 0. \tag{4.72}$$

At the final stage, separation of real and imaginary parts will give the the amplitude-phase relation. The following equations are obtained for both the amplitude a and the phase γ.

$$\dot{a} = -\delta\frac{a}{2\omega} + \frac{f}{2\omega^2}\sin\gamma \tag{4.73}$$

$$\dot{\gamma} = \sigma - \alpha\frac{10}{32}\frac{a^4}{\omega^2} + \frac{f}{2a\omega^2}\cos\gamma \tag{4.74}$$

It turns out the value of $|\omega| = 1$ according to Eq. (4.55)

4.3. Comparison with cubic-quintic Duffing oscillator

Up to now, only the quintic (fifth power α) non-linearity is studied. By considering such case, We assumed the cubic non-linearity (say ψ) is chosen to be zero. The one dimensional potential function of a quantum dot experiencing a duffing non-linear force is a Taylor expansion of the following form:

$$V(x) = \frac{1}{2}\beta x^2 + \frac{1}{4}\psi x^4 + \frac{1}{6}\alpha x^6 + ... \tag{4.75}$$

The aim in this section to take the potential function till the fifth power of non-linearity without neglecting any other terms. The outcomes will be compared to the special case ($\psi = 0$) and conclusions can be made on such assumption.

The duffing equation becomes:

$$\ddot{x} + \delta\dot{x} + \beta x + \psi x^3 + \alpha x^5 = \gamma \cos \omega t \tag{4.76}$$

The Averaging method is used and the Van der Pol transformation are applied again for the change of basis. The solving steps are therefore the same except for the additional ψ term.

After applying averaging to eliminate big angles we get the following expressions spanned by the basis vectors (u, v):

$$\dot{u}\omega = v\omega^2 - \delta u\omega - \beta v - \frac{3}{4}\psi(u^2+v^2)v - \frac{5\alpha}{8}(u^2+v^2)^2 v \tag{4.77}$$

$$\dot{v}\omega = -u\omega^2 - \delta v\omega + \beta u + \frac{3}{4}\psi(u^2+v^2)u + \frac{5\alpha}{8}(u^2+v^2)^2 u - \gamma \tag{4.78}$$

rewriting the solution in polar coordinates (r, ϕ) yield:

$$\dot{r} = \frac{-1}{\omega}\big(\delta\omega r + \gamma \sin\phi\big) \tag{4.79}$$

$$\dot{\phi} = \frac{1}{\omega}\Big(-\Omega + \frac{3}{4}\psi r^2 + \frac{5\alpha}{8}r^4 - \frac{\gamma\cos\phi}{r}\Big) \tag{4.80}$$

for steady state solutions $(\dot{r}, \dot{\phi} = (0,0))$ we obtain a polynomial expression of the form:

$$A\omega^4 + B\omega^2 + C \tag{4.81}$$

The exact values of the coefficients are:

$$A = r^2 \tag{4.82}$$

$$B = \delta^2 r^2 - \frac{3}{2}\psi r^4 \frac{5}{4}\alpha(r^6) - 2\beta r^2 \tag{4.83}$$

$$C = -\gamma^2 + \frac{25\alpha^2}{64}r^{10} + \frac{5}{4}\alpha\beta r^6 + \beta^2 r^2 + (\frac{3}{4}\psi)^2 r^6 + \alpha\psi\frac{15}{16}r^8 + \beta\psi\frac{3}{2}r^4 \tag{4.84}$$

Note that when $\psi = 0$ we obtain the result for the quintic oscillator we derived earlier using the average method.

5

Results and discussion

In the previous sections the expressions are derived using both averaging and perturbation method. To gain an understanding of these expressions, numerical simulations must be performed in order to analyse the behaviour of the dynamical system and to compare the results with the literature research.

First, The amplitude-phase relation of the quintic Duffing oscillator will be plotted for several parameter inputs. Since ω is a polynomial of fourth power, we would expect four solutions. This is indeed the case and can be seen form the plots.

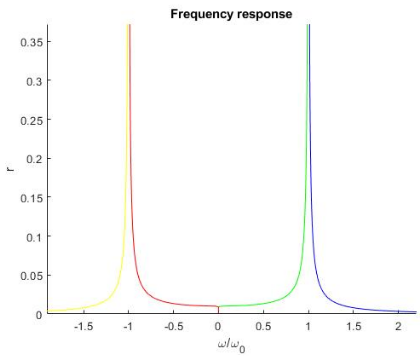

Figure 5.1: Amplitude-phase relation, values of $\alpha = 0$,$\psi = 0$, $\beta = 1$, $\delta = 0.01$,$\gamma = 0.01$.

Fig. 5.1 shows four solutions, each one corresponds to a line. It appears that the third and fourth solution is a mirroring of the first and second one relative to the r axis. This behaviour turns to be the case in all plots. The focus will mainly be on ω_1 and ω_2, therefore the other two solutions can be neglected.

$$\omega = \sqrt{\frac{-B \pm \sqrt{B^2 - 4AC}}{2A}} \geqslant 0. \tag{5.1}$$

This reduces Fig. 5.1 to the following plot:

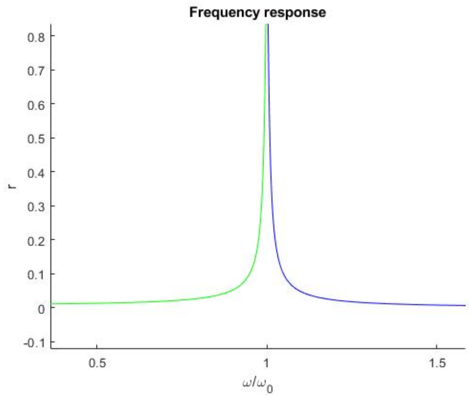

Figure 5.2: Amplitude-phase relation, only positive values of ω are shown.

In Fig. 5.2, the forced linear system is represented. The lorentzian line shape is obtained as expected. Since non-linearity is absent, there is no distortion in the shape of the lorentzian. Output frequencies are normalized to the resonance frequency $\omega_0 = \sqrt{\beta}$, and when $\omega = \omega_0$ the amplitude grows rapidly and results in Resonance which is a clear observation in many systems.

Before the fifth power parameter α is analysed, The third power ($\psi \neq 0, \alpha = 0$) will be reviewed in order to make some conclusions of the shape of the graph and to compare it to the literature. The following figure represents the amplitude-phase relation of the cubic Duffing oscillator:

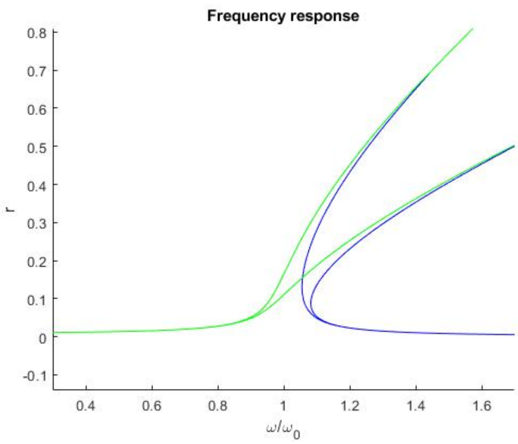

Figure 5.3: Hardening cubic Duffing oscillator.

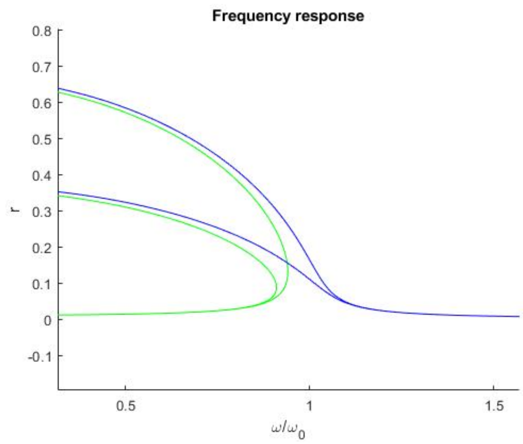

Figure 5.4: Softening cubic Duffing oscillator.

Fig. 5.3 and Fig. 5.4 represent a cubic non-linearity for respectively a hardening and softening oscillator. The first remark is the distortion of the lorentzian shape due to non-linearity. Such distortion leads to unstable solutions for different values of ω. Since the non-linearity is of third power, three r values are expected for a certain ω in some region. This can be seen by the vertical line test, which shows 3 solutions for certain frequency value. Two solutions are stable and the third on is unstable (saddle) for frequency region greater than 1. For both hardening and softening cases, the lorentzian shape becomes more distorted when increasing the magnitude of ψ.

Moving to the case of quintic non-linearity ($\alpha \neq 0, \psi = 0$), one would expect a region for which five solutions are present. The following figure shows several plots for fixed non-linearity magnitude and increasing damping coefficient:

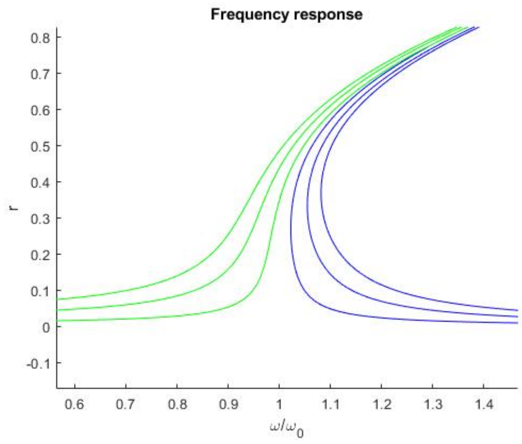

Figure 5.5: Hardening quintic Duffing oscillator, vaying damping coefficient.

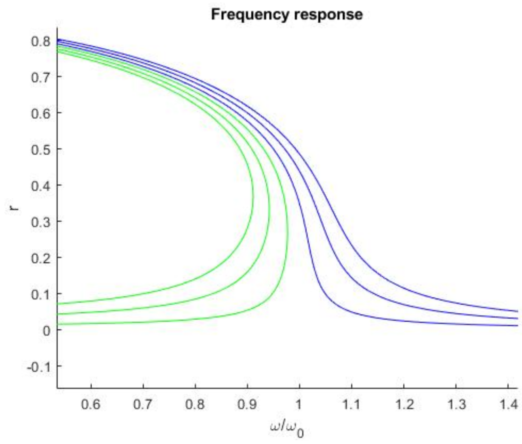

Figure 5.6: Softening quintic Duffing oscillator, vaying damping coefficient.

Both hardening and softening plots represents unexpected behaviour. Instead of five solutions, only three are present for certain frequency region(s). In both Fig. 5.5 and Fig. 5.6, The inner graph represents the smallest damping coefficient $\delta = 0.01$ and the outer graph represents the biggest damping magnitude $\delta = 0.05$. When analysing different damping values, it can be seen from the graph that for greater damping, less unstable solutions are present. Increasing the value of α will lead to the same effect as when ψ is increased. The lorentzian will become more distorted in general.

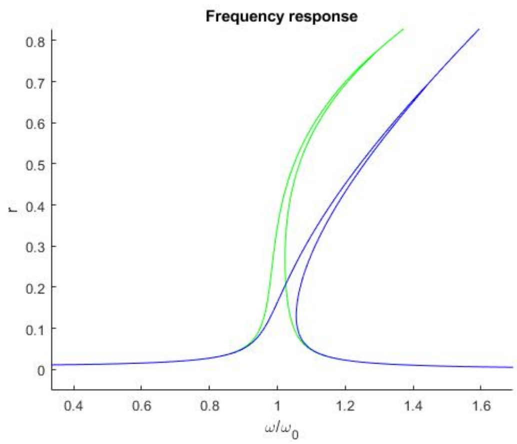

Figure 5.7: Fifth power (green),Third power (blue).

Comparing the quintic (green graph) to the cubic (blue graph) oscillator in Fig. 5.7, one can see bigger region of unstable solutions in the case of fifth non-linearity. This is the case for frequency values approx. $1.03 \leq \omega \leq 1.08$.

Further investigation in Fig. 5.8 shows that decreasing the natural frequency β causes more unstable region in the output values. This is calculated by fixing the non-linearity parameter and varying the input frequency.

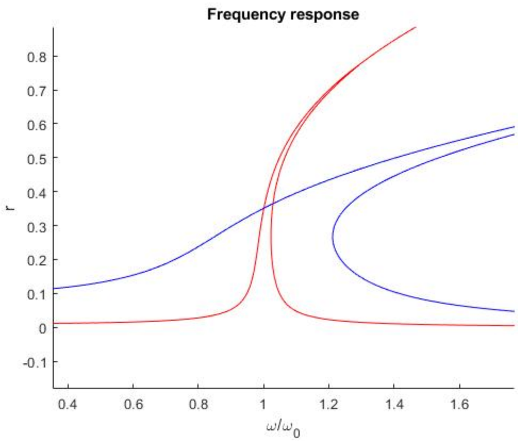

Figure 5.8: The blue line ($\beta = 0.1$) shows less unstable solutions compared to the red one ($\beta = 1$).

In the previous cases the external force is kept constant. A small change of input force requires a big amount of non-linearity change for compensation. In general the Damping coefficient seems to play the most important role for increasing stability in the system.

Before the general case ($\alpha, \beta \neq 0$)is investigated, a comparison between the average and the perturbation method will be presented. Form the calculations it was clear that both methods are in agreement with each other. The next step of verification is by comparing their numeral outcomes. This is represented in Fig. 5.9:

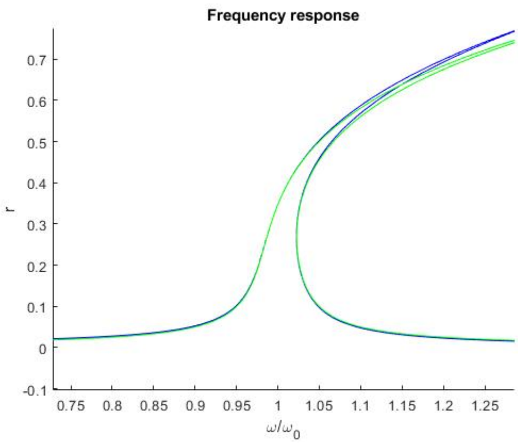

Figure 5.9: Method comparison: Averaging (blue) and perturbation (green).

The two graphs are nearly identical for frequencies in the neighbourhood of ω_0. For larger frequencies (hardening system $\alpha > 0$), the graph obtained from averaging has larger amplitude values. For the softening system, The results will be the same except that for smaller frequencies, larger amplitude values are expected for the averaging graph.

At last, The quintic-cubic Duffing oscillator will be investigated. The four following cases are studied:

1. $\alpha, \psi > 0$
2. $\alpha, \psi < 0$
3. $\alpha > 0, \psi < 0$
4. $\alpha < 0, \psi > 0$

When both non-linearities are positive case 1, the system is said to be purely hardening. To have a better understanding consider the following figure:

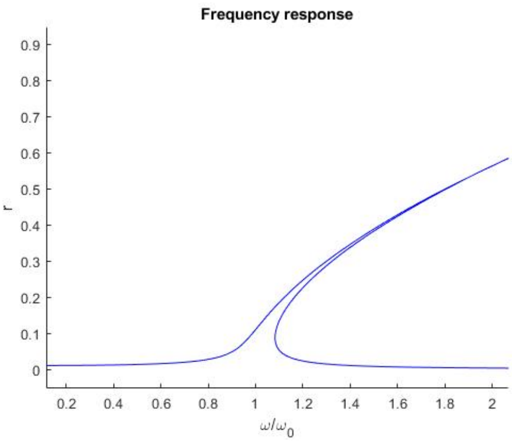

Figure 5.10: Hardening system, $\alpha, \psi > 0$.

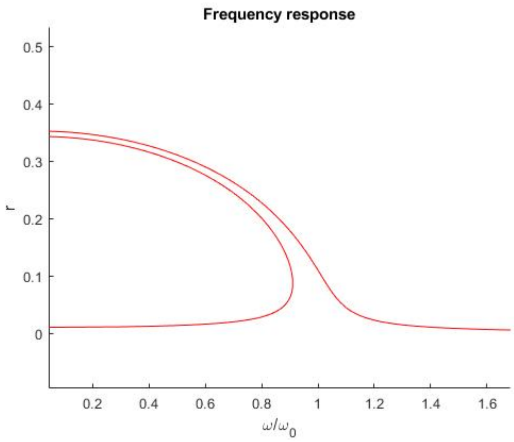

Figure 5.11: Softening system, $\alpha, \psi < 0$.

The first two cases do not seem to provide additional useful information, since Fig. 5.10 and Fig. 5.11 behave the same way as the previous cases.

For case 3, α is chosen to be $+10$ and $\psi = -3$. The reason for different magnitudes choice will become clear later. The following graph represents case 3:

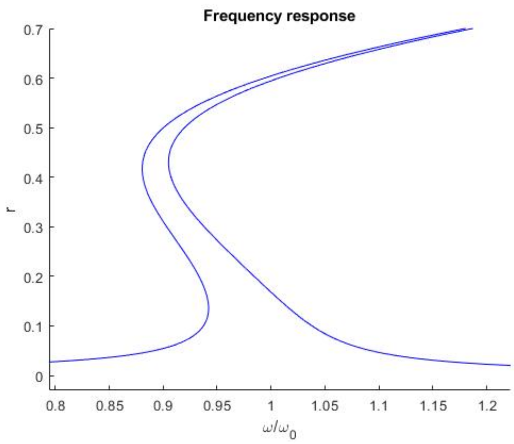

Figure 5.12: Quintic-cubic Duffing oscillator, $\alpha = +10, \psi = -3$.

Fig. 5.12 shows remarkable behaviour. For frequencies in the neighbourhood of the natural frequency, five solutions are present (three stable and two unstable). The system starts to behave as a softening oscillator due to cubic non-linearity and for large ω values, the quintic non-linearity takes over and the system becomes a hardening oscillator.

Case 4 is expected to start as a hardening system and ends as a softening one for small frequency values. Fig.15 shows the behaviour of such oscillator:

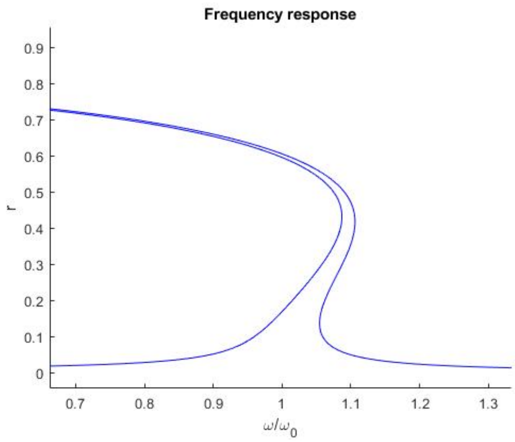

Figure 5.13: Quintic-cubic Duffing oscillator, $\alpha = -10, \psi = +3$.

In general, Case 3 and 4 are always obtained except for $|\alpha| \gg |\psi|$ or vice versa. However, in case 3 When ($|\psi| > |\alpha|$), the softening behaviour of the system will be present for more frequency values in the neighbourhood of the natural frequency. This happens also for case 4, where the opposite behaviour occurs. This behaviour is illustrated in Fig. 5.14:

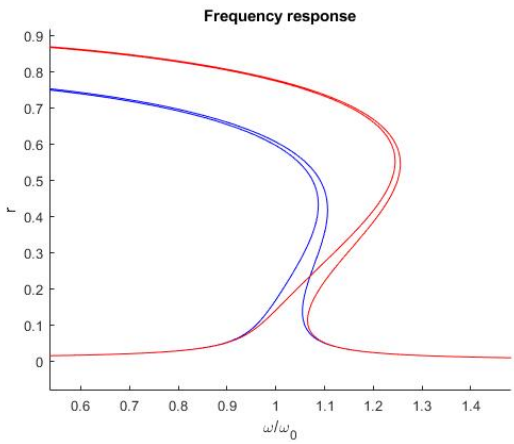

Figure 5.14: 1. $\alpha = +10, \psi = -3$ (blue) 2. $\alpha = +10, \psi = -5$ (red).

The additional input parameters such as damping and external force will have the same effect on the general case ($\alpha, \psi > 0$). Unstable solutions are always present so long non-linearity is unequal to zero. Since all cases are presented and behaviour is discussed, conclusions can be drawn.

6

Conclusion

To conclude, frequency response relation for the general case obtained by averaging is in agreement with the literature. If the quintic non-linearity is to vanish, the system is reduced to the simplified Duffing model with only cubic non-linearity. In the case of quintic non-linearity, the amplitude-phase relation fails to produce five solutions for certain frequency values.

While both cases produce unstable solution, the region of unstabilty is greater for the quintic non-linearity. This is shown by plotting both models while keeping the additional parameters such as damping, external force fixed. Increasing damping results in less unstable solutions while increasing the natural frequency of the system results in a bigger region of unstable solutions. Another consequence of varying the natural frequency input parameter is the distortion of the lorentzian shape line. Non-linearity is responsible for distortion the lorentzian shape. Varying input parameters by an absence of non-linearity will always result in symmetric lorentzian curve around the resonance frequency.

Perturbation methods succeeded in producing an amplitude-phase relation similar to the one obtained by averaging. Comparing both method with the numerical calculations show high level of agreement. For large frequency values, the curve obtained by perturbation have smaller amplitude values. The stronger the non-linearity, the greater difference in amplitude values can be expected in the perturbation curve.

For first order perturbation, The Lindsedt-Poincaré technique is reduced to the classical multiple scales method. The reason for this is due to the single non-linear parameter in the Duffing equation. For two non-linear parameters, one expects a non zero first order frequency value, which will results in different outcomes for both methods. Eliminating secularities is done for both unbounded terms which will result in unphysical behaviour and for imaginary parts.

In order to observe five solutions for fifth power non-linearity, both non-linearities must be present. Numerical calculations show that in addition to the sign of the duffing parameters, the magnitude plays a role in maintaining a region of unstable solutions. For both positve or negative valued cubic-quintic non-linearities, purely hardening and softening systems are observed. When the signs are opposite, the range in magnitude difference results in partially hardening/softening behaviour. In such case, five (of which two unstable) solutions can be observed. If there is big difference in magnitude values between both non-linearities, the system is reduced to either a purely hardening or softening system which results in only three (of which one unstable) solutions. At this final stage, an answer is given to the research question which is addressed at the beginning of this thesis.

Bibliography

[1] H. B. Meerwaldt,* G. Labadze, B. H. Schneider, A. Taspinar, Ya. M. Blanter, H. S. J. van der Zant, and G. A. Steele, PHYSICAL REVIEW B 86, 115454 (2012).

[2] Takashi Kanamaru (2008) Duffing oscillator. Scholarpedia, 3(3):6327, Duffing oscillator Scholarpedia.

[3] P.J. Holmes and D.A. Rand , The bifurcations of Duffing's equation: An application of catastrophe theory, Journal of Sound and Vibration, 44, 237-253, 1976.

[4] C. Hayashi 1964 Non-linear Oscillations in Physical Systems. New York: McGraw-Hill Book Company.

[5] J. Guckenheimer and P. Holmes, Nonlinear Oscillations, Dynamical Systems, and Bifurcations of Vector Fields, Springer-Verlag, 1983.

[6] A. H. Nayfeh and D. T. Mook, Nonlinear Oscillations, John Wiley and Sons, New York 1979.

[7] A. H. Nayfeh, Introduction to Perturbation Techniques, John Wiley and Sons, New York 1981.

[8] E. J. Hinch, Perturbation Methods, Cambridge University Press, New York 1991.